# Vibrational Superexchange Mechanism of Intramolecular Vibrational Relaxation in (CH<sub>3</sub>)<sub>3</sub>CCCH Molecules

## A. A. Stuchebrukhov, A. Mehta, and R. A. Marcus\*

Arthur Amos Noyes Laboratory of Chemical Physics,† 127-72, California Institute of Technology, Pasadena, California 91125

Received: June 24, 1993; In Final Form: August 17, 1993\*

Quantum calculations are reported for the dynamics of intramolecular vibrational energy redistribution of the acetylenic CH stretch in  $(CH_3)_3$ CCCH molecules. This paper is an extension of our previous publication (J. Chem. Phys. 1993, 98, 6044) where the line widths of the CH overtone transitions were calculated in several molecules of a general class  $(CX_3)_3$ YCCH, and it was found that the relaxation is due to a sequence of many weak off-resonance vibrational transitions between tiers of directly coupled states. The coupling of the CH stretch to a manifold of quasi-resonant states resembles the superexchange mechanism of coupling between donor and acceptor states in long-distance electron-transfer reactions. An analysis based on total population in each tier is introduced. The very rapid decrease of this population in the intermediate tiers with tier index provides evidence that the relaxation dynamics occurs via tunneling (vibrational superexchange) under a dynamic barrier in the tier space of the system. Details of the time evolution of the population under the dynamic barrier in the course of relaxation are described. "Dead end" states, their effect on the time-evolution and on spectra, their removal via inclusion of additional anharmonicities, and, thereby, their probable artificial nature in the present case are discussed.

#### I. Introduction

In the previous paper of this series, quantum calculations of homogeneous line widths of the acetylenic CH vibrational states in  $(CX_3)_3YCCH$  molecules, where X = H, D and Y = C, Si, were reported. The line widths, which provide a measure of the rate of intramolecular vibrational relaxation (IVR), result from the vibrational coupling of the acetylenic CH stretch to the rest of the molecular vibrational degrees of freedom. The study was motivated by the recent experimental results of Scoles, Lehmann, and collaborators. For these molecules extremely narrow vibrational lines, fwhm =  $10^{-1}$ - $10^{-2}$  cm<sup>-1</sup>, have been observed. In the present paper the relaxation dynamics of the acetylenic CH stretch in  $(CH_3)_3CCCH$  is explicitly studied in real time.

We summarize first some deductions of the previous study. In ref 1 it was found that the unusually slow relaxation (of the order of a hundred picoseconds), corresponding to the extremely narrow line widths in those molecules, is due to the absence of direct low-order Fermi resonances. Very high order resonances are available, but the direct coupling to such states was argued to play a negligible role: In those high-order quasi-resonant states many vibrational quanta of low-frequency modes are excited, and they can be qualitatively thought of as being separated a large distance from the light state in the state space, or classical action space, of the system. Instead of that direct coupling mechanism, the relaxation was assumed to occur in a sequence of many virtual transitions between tiers of directly coupled states, whereby the system uses the best "resonances" available, i.e., resonances typically with large detunings, to reach the final quasiresonant states. These detuned, or virtual, resonances play the role of a bridge between the initially excited state and the quasicontinuum of well resonant states. The number of sequential virtual transitions required can be as large as 10 or more in this treatment.

Such a coupling scheme resembles the superexchange mechanism of the coupling of electronic states in long-distance electron transfer in biological systems. For this reason it can be called vibrational superexchange. The very idea of superexchange as

a mechanism of indirect quantum mechanical coupling is very general and has been discussed in the literature for a long time.<sup>5</sup> The difference between the usual electronic superexchange and vibrational superexchange is that in the former case the quasi-resonant electronic states of donor and acceptor, coupled indirectly via many virtual transitions, are separated by barriers in coordinate space while in the latter case the CH vibration and the quasi-resonant states, where many vibrational quanta of low frequency modes are excited, are separated in the action space, or in the zeroth-order quantum number space, of the system.

A tier of states is defined by the total number of quanta that each state in the tier differs from the light state, as described below. (The light state constitutes the n = 0 tier.) The population of the *n*th tier,  $P_n(t)$ , is a sum of the population of all states belonging to that tier. In many cases, the relaxation dynamics of the light state, the so-called survival probability, is studied.<sup>6–8</sup> This function can be most easily calculated and experimentally probed. In the present case such a strategy would correspond to the calculation of population of only the CH vibration,  $P_0(t)$  in our notation. In addition to  $P_0(t)$ , the populations of other tiers  $P_n(t)$ , n = 1, 2, ..., are also studied in this paper. The population of each of the higher tiers provides, in fact, the main insight into the relaxation process. We consider not only how the relaxation of excitation of the CH stretch occurs but also how this excitation spreads over the other vibrational states in the molecule. Several authors in the past have recognized the importance of the analysis of the population of the dark states.6,7,9-11

Two limiting quantum mechanical forms of intramolecular vibrational relaxation (IVR) can be envisaged, using a zeroth-order basis set description: In one of these there would be a successive set of vibrational energy transfers, each governed by a kinetic expression, to near-resonant states, and so the overall transfer would be governed by a master equation. Any coherence would be completely lost at each step. In a second limiting mechanism the energy transfer would proceed from the initial zeroth-order state to a final near-continuum set of quasi-resonant states via a series of transitions over off-resonant states. These states are the virtual states mentioned above. This latter mechanism can appropriately be called vibrational superexchange, as noted above. In the present paper we describe results for the

<sup>†</sup> Contribution no. 8815.

<sup>•</sup> Abstract published in Advance ACS Abstracts, December 1, 1993.

IVR of the (CH<sub>3</sub>)<sub>3</sub>CCCH molecule in which the acetylenic CH is prepared in its first excited vibrational state.

There are certain analogies to a classical, or really to a semiclassical description, 12,13 in that the off-resonant superexchange mechanism could correspond to a "dynamical tunneling": In the molecule, invariant tori in phase space are associated with the zeroth-order classical action variables and correspond semiclassically to the zeroth-order quantum states all in a manydimensional, nearly parabolic energy well. If the introduction of the perturbation resulted only in the distortion of these tori but not their destruction, then extensive IVR could occur by a "dynamical tunneling" from one torus to the next, as described by Davis and Heller.14 ("Tunneling" between tori has been extensively investigated, in one way or another, by a number of researchers since the early seventies. 15) In an actual classical mechanical system with many coordinates, such as the present one, one can expect that the invariant tori will be at least partially ruptured and that another mechanism involving the chaotic-like passage through these fragments can occur classically and has been discussed by various authors.16

For this reason, we believe that the simplest quantitative description of the IVR process in these many-dimensional systems is the quantum mechanical one, though there will be an analogy between the vibrational superexchange mechanism and a tunneling between the zeroth-order invariant tori.

In the present paper the concept of tier population is introduced, converting the results of the many-coordinate IVR problem to a one-dimensional visualization. The presence of "dead-end" states, their effect, and their possible removal when higher order anharmonicities are introduced, are also discussed. A comparison is made with crude phenomenological descriptions of the successive incoherent steps mechanism and of the vibrational superexchange mechanism, using the long-time behavior.

The structure of the paper is as follows. In section II some theoretical aspects of the tier model are discussed and in section III dynamics of the tier system of (CH<sub>3</sub>)<sub>3</sub>CCCH molecule is studied. In section IV, the results are discussed.

#### II. Tier Model

Statistical IVR is usually understood as the relaxation of the state that is directly accessible from the ground state through a transition moment, the "light state", into a large number of anharmonically coupled "dark" states which are inaccessible from the ground state. This coupling arises from the deviation of the potential surface, written in normal mode or normal mode/local mode coordinates, 17 from harmonic behavior. A refinement of this model divides the dark states into various tiers. 1 Each state in a given (nth) tier is coupled through third-order anharmonic couplings to states in the n-1 or n+1 tiers. If fourth-order couplings are being taken into consideration, then the states in the *n*th tier are coupled to states in the n-2 and n+2 tiers. Once the light state is specified, the tiers are then created sequentially. The cubic (or quartic) anharmonicity operator is written in terms of creation and annihilation operators which act on the light state to generate the first tier, on the first tier to generate the second tier and so on until some specified criterion (usually, the number of states) is met. Care is taken to avoid duplication of states in different tiers in this scheme, a scheme which is implemented naturally in C language with dynamic memory management and the use of pointers.1 The first six tiers for (CH<sub>3</sub>)<sub>3</sub>CCCH, generated in this way with a model potential anharmonic field developed in ref 1, are shown in Figure 1.

Once the tier structure is complete then the complete  $N \times N$  vibrational Hamiltonian is formed within this basis set and analyzed. The Hamiltonian is diagonalized using the standard algorithms for complete diagonalization of large, sparse symmetric matrices. Upon diagonalization the eigenvectors are normalized. This procedure of exact and complete diagonalization has a built-in limitation on the size of the matrix. For example, with access

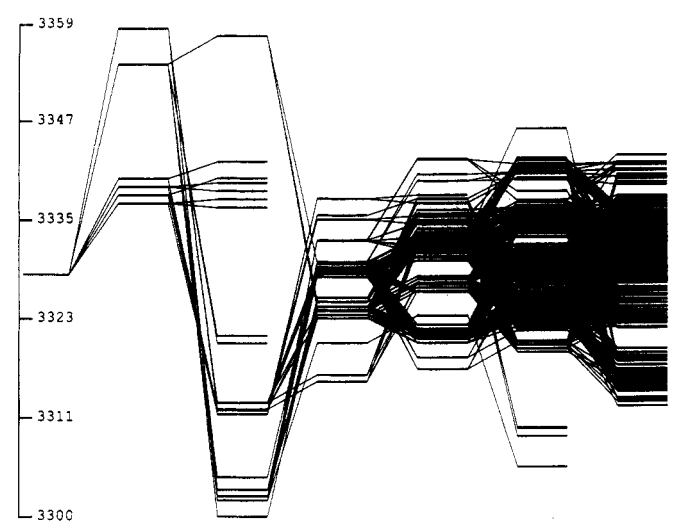


**Figure 1.** First six tiers of sequentially coupled zero-order states in  $(CH_3)_3$ -CCCH. The first state on the left is the acetylenic CH vibration v = 1.

to 10 Mwords = 80 Mb of memory on our computer, memory constraints limit the dimension of the matrix to  $\approx$ 2000. Use of Lanczos-type ideas for diagonalization may be useful in dealing with larger matrices. Further details on the generation of the tier structure and the associated computational details are given in the previous paper in this series.\(^1

Having calculated the eigenvalues,  $E_i$ , and the eigenvectors,  $|\psi_i\rangle$ , it is possible to perform the dynamics calculations on all the zeroth-order states. The transition intensities of different lines in the absorption spectra can also be obtained. The spectrum shows how the single line of the transition to the light state splits into a broadened band of transitions in the presence of the anharmonically coupled dark states. The absorption spectrum is related to the amplitude of survival probability of the light state  $(|\phi_0\rangle)$ , which is defined as

$$p_0(t) = |\langle \phi_0 | \phi(t) \rangle|^2 = |\langle \phi_0 | e^{-i\hat{H}t} | \phi_0 \rangle|^2$$
 (1)

where  $|\phi(t)\rangle$  is the state evolving in time from the prepared state  $|\phi_0\rangle$ . The Fourier transform of  $\langle \phi_0|\phi(t)\rangle$  is given by

$$I(\omega) = (1/2\pi) \int_{-\infty}^{\infty} \langle \phi_0 | \phi(t) \rangle e^{-i\omega t} dt$$
 (2)

Here,  $I(\omega)$  is proportional to the actual absorption spectral lineshape, as defined in ref 18. One factor in the proportionality constant is the square of the dipole transition moment. Inserting the resolution of the identity

$$1 = \sum_{i=1}^{N} |\psi_i\rangle\langle\psi_i| \tag{3}$$

(the  $\{\psi_i\}$  form a complete set of orthonormal eigenvectors within this basis) and using  $\hat{H}[\psi_i\rangle = E_i[\psi_i\rangle$ , we have

$$p_0(t) = |\sum_{i=1}^{N} |\langle \phi_0 | \psi_i \rangle|^2 e^{-iE_i t}|^2$$
 (4)

$$I(\omega) = \sum_{i} |\langle \phi_0 | \psi_i \rangle|^2 \delta(\omega - E_i)$$
 (5)

Similarly, the population of any other zeroth-order state  $\phi_j$  is given by

$$p_{j}(t) = |\langle \phi_{j} | \phi(t) \rangle|^{2} = |\langle \phi_{j} | e^{-i\hat{H}t} | \phi_{0} \rangle|^{2} = |\sum_{i=1}^{N} \langle \phi_{j} | \psi_{i} \rangle \langle \psi_{i} | \phi_{0} \rangle e^{-iE_{i}t}|^{2}$$
(6)

To obtain insight into the mechanism of IVR the actual dynamics of each of the invidual zeroth-order states has been calculated.

Since the total number of states is so large, a global picture of the dynamical behavior of the molecule was obtained from the dynamical behavior of each state by calculating the total population in a given tier as a function of time:

$$P_n(t) = \sum_{k=1}^{N_n} p_k \tag{7}$$

where  $N_n$  is the number of states in the *n*th tier and the  $\{|\phi_k\rangle\}$ belong to the *n*th tier.  $P_n$  is the total population in the *n*th tier. In the zeroth-tier there is only one state, the light state, making  $p_0(t) = P_0(t)$ . With these tools available for the analysis, the dynamical behavior of the tier model can be examined in detail.

#### III. Dynamics of the Tier System

3.1. Reduced Dynamics with a Quasi-continuum Tier. The detailed analysis of the relaxation mechanism in (CH<sub>3</sub>)<sub>3</sub>CCCH is presented next. For this molecule a total of about 30 000 states, sequentially coupled to the light state, were identified in an artificial intelligence search procedure using a perturbation theory based criterion. 1 Only those states that are expected to contribute significantly to the relaxation process are included in the calculation. The first six tiers of this system are shown in Figure 1. The whole structure contains detailed information about the relaxation pathways.

To study the dynamics of such a huge system some simplification has been adopted, because the total system cannot be diagonalized exactly. For this reason, only 10 tiers of the real system which contain 624 states are included in the present calculation. Then, to stimulate the presence of the quasicontinuum of other states in the later (>10) tiers and yet to stay within the limits of possible complete diagonalization, an eleventh tier is added within a narrow resonant energy window taking the total number of states to 2000, the energy of each state in the eleventh tier being random within a prescribed window. This number is the maximum number of states that can be diagonalized directly in the computer being used, due to memory constraints.

This eleventh tier phenomenologically describes the prediagonalized states from all the actual tiers with numbers n > 10. The energy window for this, the eleventh, tier was chosen to be 0.5 cm<sup>-1</sup> around the major peak in the spectrum of the 10-tier system. This major peak is slightly shifted from the energy of the light state due to its interaction with the other states. The additional states in the eleventh tier are coupled randomly with states in the tenth tier. The matrix elements between states in tier 10 and tier 11 form a Gaussian distribution centered at the energy of the main eigenstate of the 10-tier system, such that any edge effects from the additional tier may be minimized. The density in the eleventh tier was chosen in such a way as to make the total density of states roughly equal to the total density of dark states for the fundamental transition of the CH stretch in the 42-dimensional oscillator model described in detail in ref 1. Although it is reasonable to expect that this last tier may impose some artifacts on the dynamics, we believe from the results below that this simplified approach, where a light state is coupled through intermediate tiers to a quasi-continuum of states, provides a realistic model of the process of IVR in (CH<sub>3</sub>)<sub>3</sub>CCCH. Before considering the details of the mechanism, it is useful to comment on the effect of the addition of this eleventh quasi-continuum tier on the dynamics and spectra.

In Figure 2 the population dynamics of the light state  $p_0(t)$ , i.e., the survival probability, is shown with and without the quasicontinuum (eleventh) tier. It is seen that while the initial (≤200 ps) relaxation of the light state is identical for the two systems, recurrences of population for the light state are present for the 10-tier system. This observation shows that during the decay in the first 200ps the higher tiers of states are irrelevant and, therefore, the initial decay is completely a local phenomenon. The same conclusion can be reached from the sum rule for the

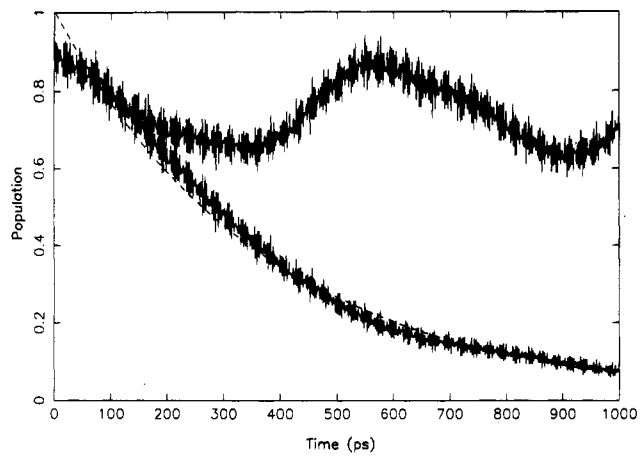


Figure 2. Top curve: survival probability of the acetylenic CH stretch in the 10-tier system without the addition of a tier to simulate the presence of a quasi-continuum. Bottom curve: survival probability of the acetylenic CH stretch when the quasi-continuum tier is present. Dashed line is the least-squares exponential fit to the bottom curve.

width of the absorption spectrum.1 This width is the inverse relaxation time for the short-time behavior.

The addition of the eleventh tier, however, changes the longtime behavior of the survival probability, significantly curtailing the long-time recurrences (Figure 2). After some initial transient behavior, the decay of the light state is exponential, as expected in a statistical limit. That  $P_0(t)$  in the two curves does not appear to approach 1.0 as  $t \rightarrow 0$  reflects a very rapid (almost instantaneous on our time scale) dilution of the light state by far off resonant interactions. Thus, we conclude that the presence of the quasicontinuum tier is essential and that more than 10 tiers are needed to describe the irreversible decay of the CH stretch.

Similar dramatic effects are observed in the absorption spectra when the quasi-continuum tier is added. For the 10-tier system, i.e., for the system without a quasi-continuum, the spectrum is shown in Figure 3a. It essentially consists of one major peak. The addition of the 11th tier with a high density of resonant states produces an effect shown in Figure 3b. It is seen that a broad distribution of peaks is formed with about the same full width at half maximum as predicted by the Golden Rule. Since the statistical decay of the population requires the presence of a high density of well resonant states, the addition of this last tier is absolutely essential.

While the addition of the eleventh (quasi-continuum) tier has transformed the spectrum from a few separated eigenstates into a well-defined band of absorption lines, the density of lines in the spectrum is still smaller than its actual value in real molecule. In our multidimensional oscillator model we have not taken into account the possibility of methyl groups tunneling between equivalent torsional positions. The tunneling events transform the  $C_{3\nu}$  point-group symmetry of our oscillator model into  $G_{162}$ molecular symmetry group, 19 significantly increasing the number of possible anharmonic couplings of the light state to the dark states. This effect was argued to increase the density of actual spectral lines: possibly by a factor<sup>2,3</sup> as large as 24.

To see what can happen with the spectrum if the density of available dark states is increased further from its present value in the quasi-continuum tier, model calculations were performed. In these calculations a single light state is randomly coupled to a tier with density of states 705 and 20000/cm<sup>-1</sup>, respectively. The former density corresponds to our oscillator model while the latter corresponds to the breaking down of the  $C_{3v}$  symmetry. The spectrum of such a model system is shown in Figure 4. The absolute energy position of the light state is not critical in this model calculation. As the density of states  $(\rho)$  is increased while  $ho \bar{v}^2$  is kept constant ( $\bar{v}^2$  is the mean square matrix element), the spectrum is transformed from a series of disconnected peaks into a Lorentzian. In Figure 4,  $\Gamma = 2\pi\rho\bar{v}^2$  is kept constant and the

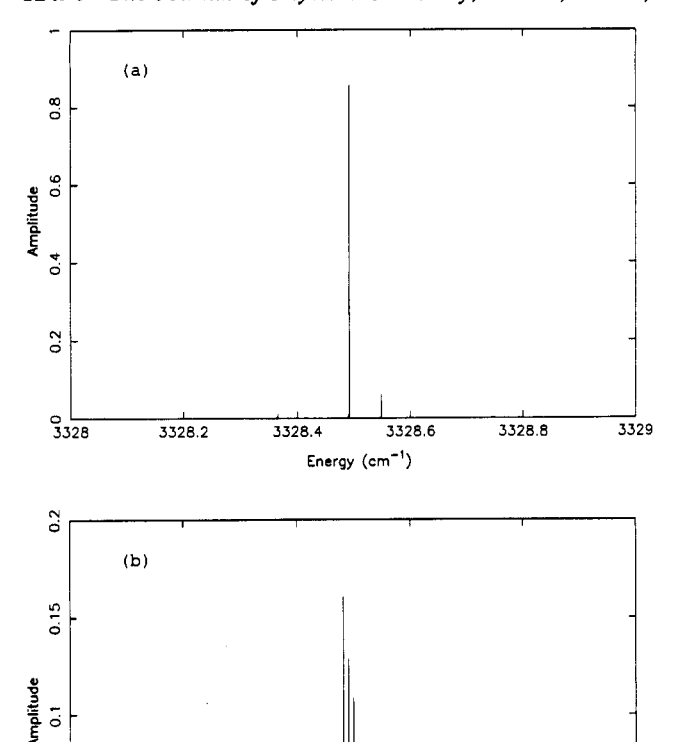


Figure 3. Absorption spectra corresponding to the (a) 10- and (b) 11-tier systems that simulate the acetylenic CH stretch in (CH<sub>3</sub>)<sub>3</sub>CCCH.

Energy (cm<sup>-1</sup>)

3328.4

simulated curve is compared to an idealized curve of Lorentzian shape with this  $\Gamma$ , this idealized curve being given by

$$I(\omega) = \frac{1}{\pi} \frac{\Gamma/2}{(\omega - \omega_0)^2 + (\Gamma/2)^2}$$
 (8)

3328.6

3328.8

where  $I(\omega)$  is the spectral absorption lineshape.

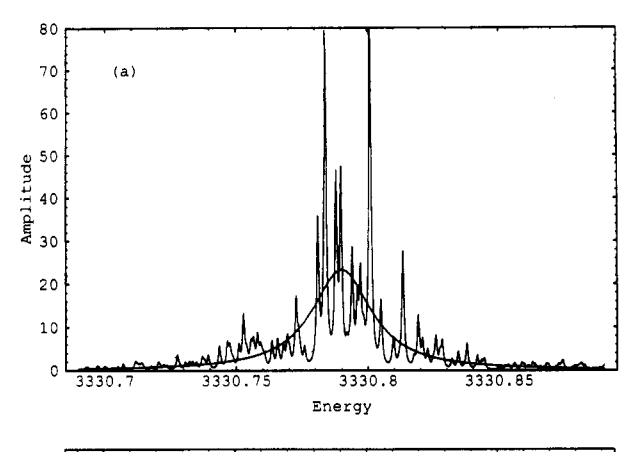
3328

3328.2

Thus, we infer that the spectrum of our model, Figure 3b, will continuously evolve into the Lorentzian envelope, observed experimentally, when the density of states in the quasi-continuum tier reaches its actual value and when account is taken of the possible experimental broadening of each individual eigenstate. Once the statistical limit is reached, any further increase in the density of states simply fills in the remaining spaces within the individual eigenstates.

We focus next on the characteristics of the dynamics of populations of tiers with tier numbers  $n \ge 1$ , i.e., on the dynamics of the accumulating population of states other than the light state.

**3.2.** Long-Time Dynamics of the Tier System. Dead-End States. The main qualitative feature of the dynamics of the tier system on the time-scale of decay of the light state is shown in Figures 5 and 6. For each tier n we again are interested in the evolution of the population of the whole tier,  $P_n$ . The time evolution of  $P_n$  shows that the population of the intermediate tiers is always very small (<0.1, Figure 5), never building up significantly. At the same time, the population of the light state decays (Figure 2) and the population of the eleventh, or quasicontinuum tier rises, apparently as a result of this decay (Figure 6). Qualitatively, it appears as if the population flows directly to the distant eleventh tier, largely bypassing the intermediate tiers. This type of behavior is typical for a superexchange mechanism. There is also an analogy to a tunneling dynamics which we discuss in the later sections in the paper.



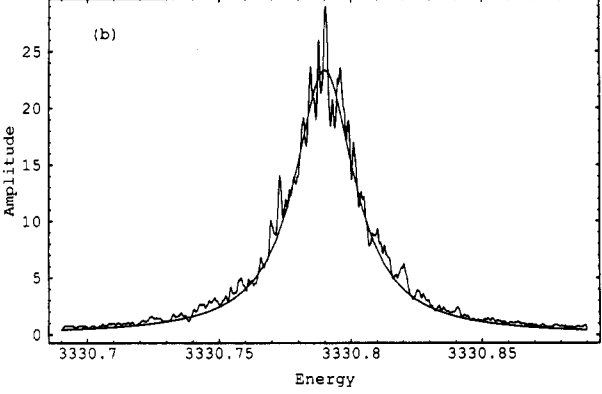


Figure 4. Spectrum of a light state *directly* coupled to a dense manifold (density =  $\rho$ ) of dark states: (a)  $\rho = 705/\text{cm}^{-1}$ ; (b)  $\rho = 20000/\text{cm}^{-1}$ .

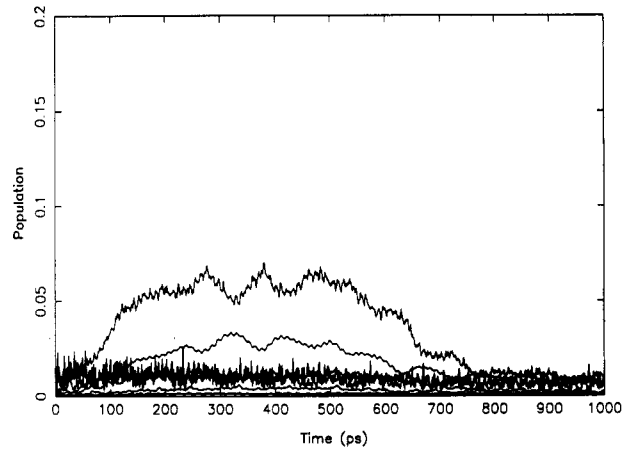


Figure 5. Population of tiers 3-10 as a function of time in the presence of the eleventh tier. The top curve is tier 5, the next is tier 9, a cluster of tiers 3, 4, and 7 are next, tier 8 is next, and a pair of tiers 6 and 10 are lowest.

The off-resonant states are virtual states, and for this reason preclude a buildup of population within the intermediate tiers (Figure 5). However, some buildup of the population is possible if by accident there is a good resonant state in a distant tier and that state is not coupled by cubic terms to further tiers in the system. We call such states dead-end resonant states. Such states are of a somewhat artificial nature, because there are always higher order anharmonic couplings. However, in calculations with a model anharmonic field, like the present one, after selecting states with an artificial intelligence search procedure in the tier system and using only third-order anharmonicities there can be such states as described above. Their effect is considered next.

It has been noticed that there are several such dead-end states in our tier system. Of such states, only two states in the third tier were found to have a significant effect on dynamics and spectra. One of these states is more resonant with the position of the absorption band than the other one and, therefore, has a

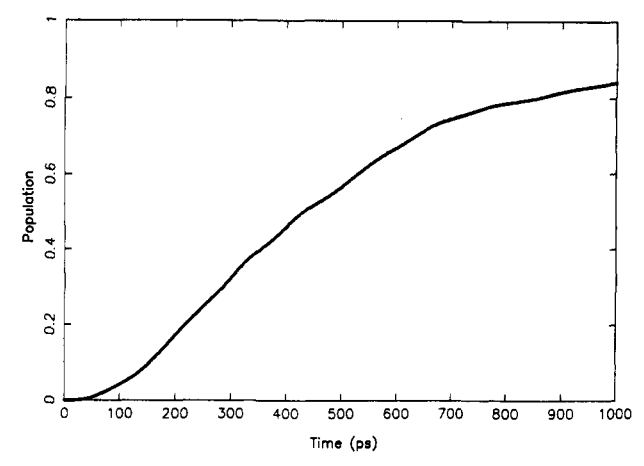


Figure 6. Time-evolution of the quasi-continuum tier in (CH<sub>3</sub>)<sub>3</sub>CCCH.

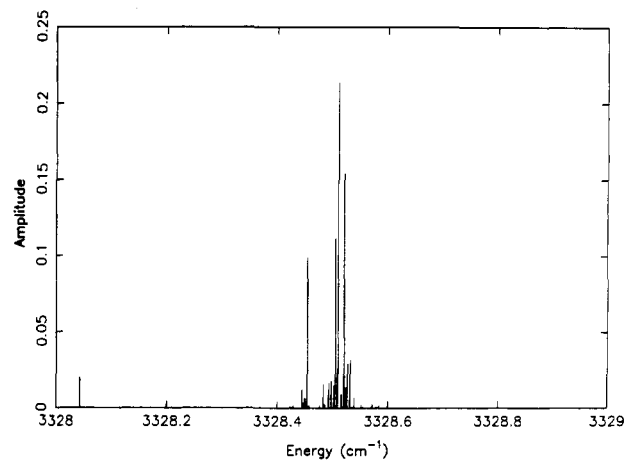


Figure 7. Spectrum when the dead-end states are added. Compare with Figure 3b.

larger effect. We also noticed (calculations given below) that the effect of these two states is considerably reduced when small quartic terms coupling them to further (n+2) tiers are introduced. Because of their artificial nature, these states have been removed from the calculations described in section 3.1. In the absence of further couplings, the removal of the dead-end states does not effect the overall IVR process dramatically, especially on a longtime scale. The calculations have also been performed in a system where such resonant dead-end states are present. These calculations are described next.

In Figure 7 the spectrum of the system with resonant dead-end states is shown. Comparison with Figure 3b shows that the deadend states produce additional components in the spectrum. These separate peaks are due to the absence of couplings of the deadend states to states in further tiers. The overall dynamics of the tier system, however, does not change qualitatively when the deadend states are present. The dynamics of the light state and the quasi-continuum tier are shown in Figure 8. As a result of a single strong resonance in the third tier, in the time evolution of the light state there is a tendency now for a coherent quantum beat to occur. There also exist fast oscillations of smaller amplitude due to the off-resonant dead-end state.

In Figure 9 the population of the third tier and the population of the resonant dead-end state is shown. It is seen that practically all the population of the tier is due to a single state. The population of the third tier is in this case significantly larger than the population in other tiers of the system because of the direct

The nearly resonant state in the third tier is not coupled further via cubic terms in the Hamiltonian, as we have already noted. Its removal does not affect the overall dynamics significantly, but it does destroy the coherence between the light state and the third tier as seen from the comparison of Figures 2 and 8. A

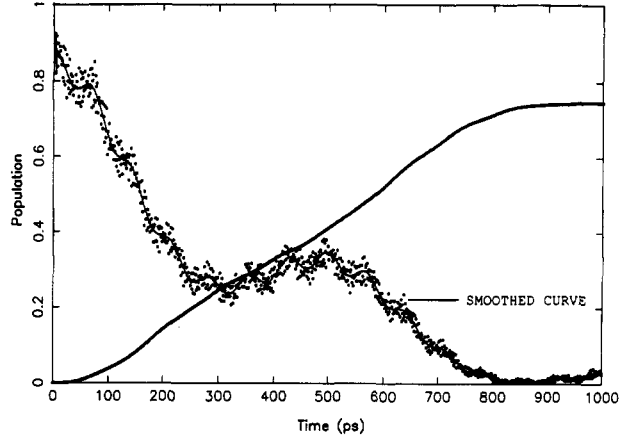


Figure 8. Survival probability (of light state) and the dynamics of the quasi-continuum tier when the two dead-end states are included. Compare with Figures 2 and 6.

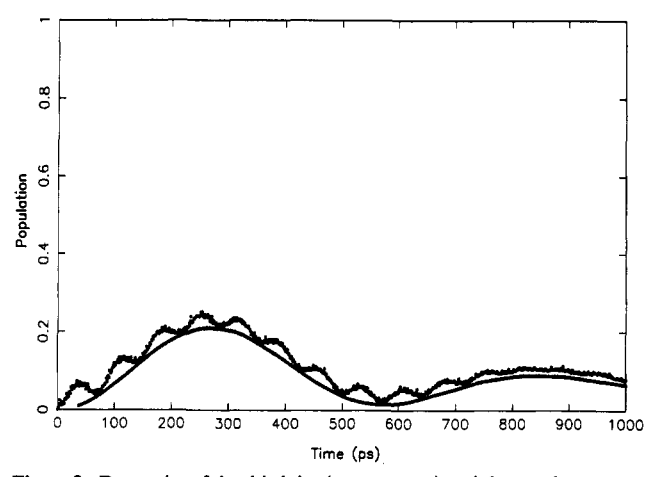


Figure 9. Dynamics of the third tier (upper curve) and the nearly resonant dead-end state (lower curve).

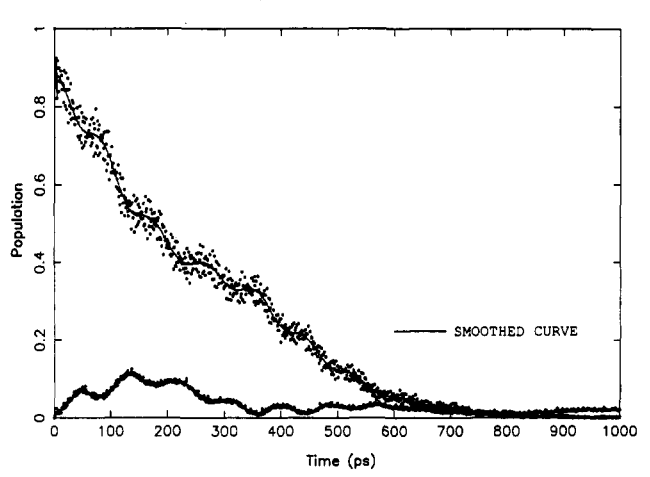


Figure 10. Survival probability of the light state (upper curve) and the dynamics of the third tier (lower curve) when the dead-end states are further coupled through quartic anharmonicities.

similar effect to this actual removal of the dead-end states can be achieved by adding higher anharmonic couplings (quartic and quintic) that have not been taken into account. To gauge the effect of additional higher order couplings, the two dead-end states (in the third tier) were coupled to a few states in the fifth tier with a quartic matrix element of 0.5 cm<sup>-1</sup>. The result is shown in Figure 10. The quantum beat behavior is significantly reduced, the coherence being destroyed by the further coupling of these two (one of them nearly resonant) dead-end states. It is, therefore, reasonable to anticipate on this basis that the states which are not coupled to further tiers by cubic terms and act in a beatlike manner with the light state will often not show such

TABLE I: Average Matrix Element v, Density of States o and Window Size for Each Tier of the Model System (Total States = 2024)

tier	window, cm-1	ρ	ō, cm⁻¹	tier	window, cm <sup>-1</sup>	ρ	<i>v</i> ̄, cm <sup>−1</sup>
1	0.2	10	0.03	6	0.2	270	0.07
2	0.2	25	0.04	7	0.2	470	0.07
3	0.2	90	0.05	8	0.2	740	0.07
4	0.2	140	0.06	9	0.2	1395	0.07
5	0.2	200	0.06	10	0.2	6775	0.07

behavior when higher-order couplings are taken into account. This result also points out that our calculations reflect accurately the gross features of the IVR dynamics and that they may contain artificial details which are sensitive to the individual positions, couplings of the states and their matrix elements in the model. Such is the case when an apparent dead-end state, arbitrarily uncoupled to further tiers, is present. The Lorentzian nature of the experimentally observed spectrum<sup>2</sup> shows the absence of such states in the actual molecule. It should be noted that in smaller molecules where there is no statistical decay, onset of IVR is denoted by splittings of individual J, K peaks and presence of quentum beats in the dynamics.

3.3. Short-Time Dynamics of Intermediate Tiers. In the tier system of the (CH<sub>3</sub>)<sub>3</sub>CCCH molecule the population of the intermediate tiers is extremely small during the relaxation process. However, those tiers provide the bridge for the population flow from the light state into the quasi-continuum of states in higher tiers. A closer examination of the dynamics of tiers reveals that the population in tiers shows an intriguing behavior at short times, providing an interesting detail of the relaxation process.

To explore further some details of the dynamics of intermediate tiers, calculations were performed on a model tier system. In this system the coupling to the light state as well as the number of states in the intermediate tiers were increased in order to make population of the intermediate tiers somewhat larger and less "noisy". Otherwise this model system qualitatively resembled the real one whose tier structure is shown in Figure 1. The population of each intermediate tier was still sufficiently small to correspond to the superexchange type of coupling rather than the overlapped resonances case: The population of tiers 2-9 never exceeded 0.2. Also, for each intermediate tier, the product of  $\bar{v}$ , the average coupling matrix element between successive tiers, and  $\rho_{\rm eff}$ , the effective density of directly coupled states, was smaller than unity ( $\approx$ 0.5). In other words, the average detuning of two coupled states was larger than the coupling matrix element. These facts confirm that the relaxation mechanism corresponds to the superexchange type of coupling behavior. The exact parameters of the model system are given in Table I.

The short-time dynamics of the first four tiers of this model system is shown in Figure 11. It is seen that at short times the population displays an interesting threshold behavior. The same kind of behavior is common to all intermediate tiers. For any given tier n, the population remains near zero before suddenly increasing. This time, when the front of the population distribution reaches tier n is denoted by  $t_c^n$ . In Figure 12 the initial population evolution for the first eight tiers is shown in greater detail. Figure 12 shows that the population distribution front moves with constant velocity along the tier coordinate. In other words,  $t_c^n$  increases linearly with tier number n, Figure 13. It may be surmised that for some initial time the bulk of the population remains localized in the initial tiers while a small portion leaks out into the intermediate tiers. The distribution function of the population in the initial stage of relaxation, when the population of the light state has not decayed significantly, develops a very thin tail in the region of the intermediate tiers. At short times this tail has a sharp front that moves with constant velocity and appears as a threshold when the dynamics of each tier is analyzed. Statistical decay occurs once this front reaches the quasi-continuum. The population then leaks from the light state into the quasi-continuum through the formed "tunnel" with a near steady state population

in each intermediate tier at some intermediate times. Of course, once the population of the bright state has decayed the population in the intermediate tiers will decrease also.

Addition of fourth-order anharmonicities may scramble the constant velocity of the sharp transition, but we may still expect a residual effect. Within the model systems it was also observed that the initial tiers become saturated very soon and for this reason probably have a different velocity than the intermediate and later tiers (Figure 13).

3.4. Superexchange or Overlapping Resonances? In principle two different limiting mechanisms could be envisaged for the dynamics of the energy flow through the sequence of tiers. In one of these there would be a successive set of real vibrational energy transfers—from the light state to the first tier, from first tier to the second one, and so forth until the quasi-continuum tier is reached. The overall transfer would be governed by a kinetic master equation. In this scheme the coherence is lost in each step of energy transfer. This type of IVR occurs when in a classical description, there is a sequence of many overlapping resonances, as described in a series of papers by Sibert et al.20

In the second type of mechanism the energy transfer would proceed from the initial state to a final near-continuum set of quasi-resonant states via a series of off-resonant transitions, with no classical overlap. This mechanism does not require a sequence of classical overlapping resonances between the light state and other states in the molecule. The intermediate off-resonance states can be only weakly coupled to a light state. This latter mechanism corresponds to superexchange.

Rigorously speaking, from the smallness of the population of the intermediate tiers one cannot distinguish between the two IVR schemes described above. Thus, although the low population in the intermediate tiers suggests that the energy transfer might be due to superexchange, the kinetic type of equations could, in principle, give a very low population distribution in the intermediate tiers. This situation can happen, for example, due to a high rate of energy transfer into quasi-continuum tier from the previous one and a small rate of transfer from the light state into the first tier. One can, however, distinguish between the two mechanisms in a different way, considered next.

To distinguish between the mechanisms and then to establish that the relaxation dynamics in the intermediate tiers indeed corresponds to a coherent superexchange mechanism, as opposed to a possible incoherent kinetic type of transitions between tiers, the quasi-stationary population (at t = 1000 ps) of the intermediate tiers is compared in Figure 14 with density of states in the tiers. (The calculation is for the "real" system rather than the model system that was employed to determine the transient behavior in section 3.3.) If the dynamics in the intermediate tiers were governed by a kinetic type of equation, the quasi-stationary population in each of the tiers would be approximately proportional to the density of states in that tier, and so would increase with tier index. Instead, as is seen from Figure 14, the quasi-stationary population decreases with tier number, as if there were a barrier separating the light state from quasi-resonant states in the distant tiers (Appendix).

From Figure 14 it is clear that, apart from some local fluctuations, the population decreases significantly with tier number. Also, (not shown) the population ratio  $P_i/P_{11}$  is continually decreasing for each tier with time. The marked decrease of population with tier number reinforces our belief that the overall mechanism of relaxation is tunnelling-like and not kinetic. If the kinetic behavior was being followed, then the population distribution should have paralleled that of the density of states and so would have increased with tier number.

### IV. Discussion

The tier system of the (CH<sub>3</sub>)<sub>3</sub>CCCH molecule shows an interesting dynamical behavior. The population in the intermediate tiers never builds up significantly, and the population

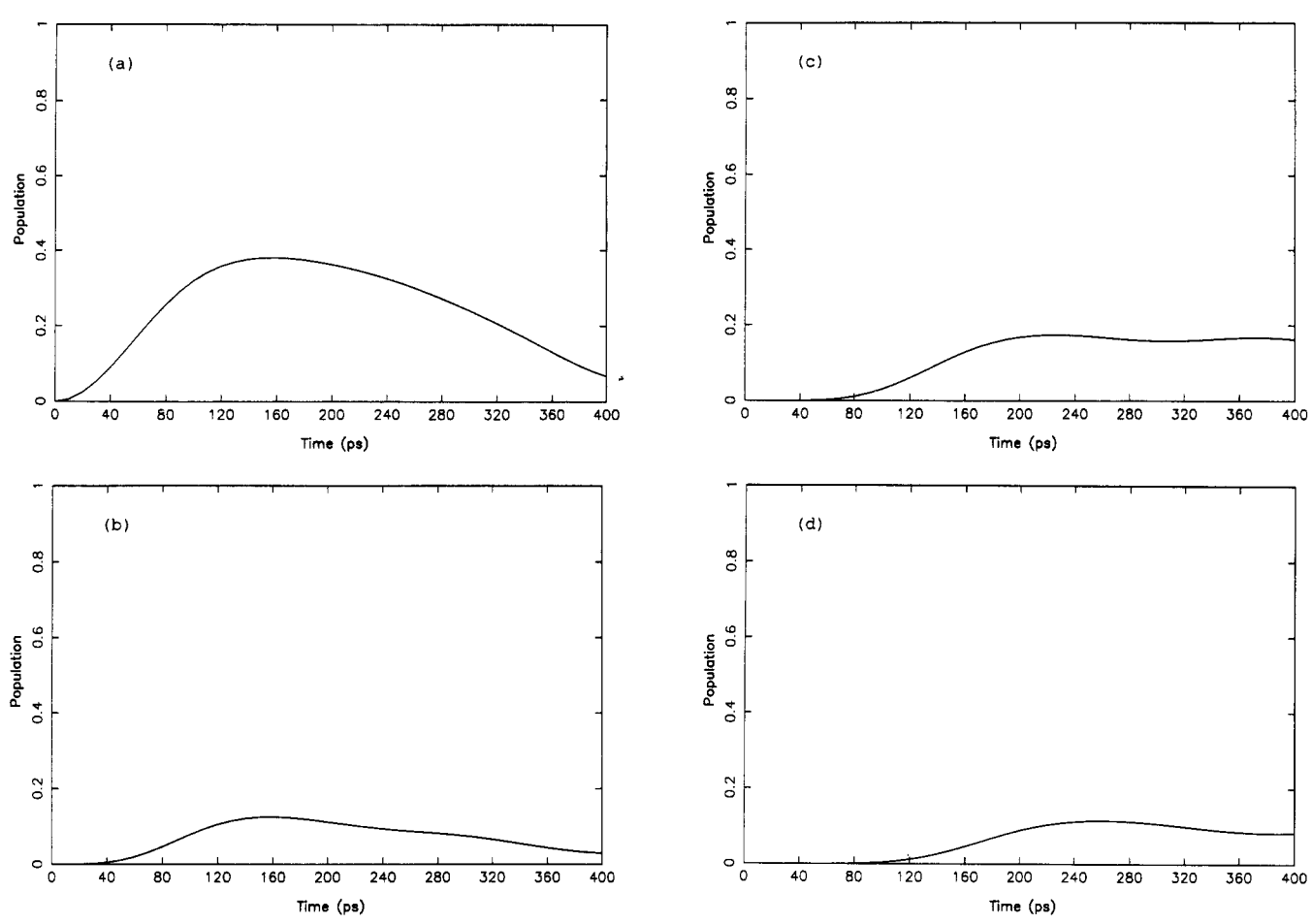


Figure 11. Population dynamics of first four tiers in a model system showing the threshold behavior: (a) first tier; (b) second tier; (c) third tier; (d) fourth tier. See text for details about the model system.

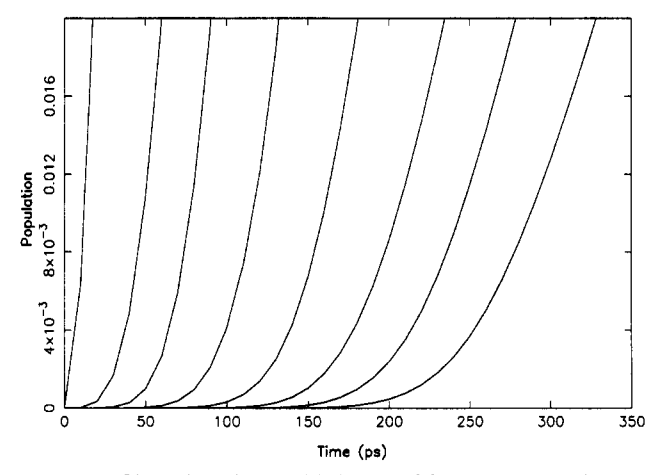


Figure 12. Short-time threshold behavior of first eight tiers of model system.

from the light state flows directly into a quasi-continuum tier, largely bypassing the intermediate tiers. The mechanism of the transfer was established to be a coherent superexchange. If the probability of finding a real particle at some discrete points along the coordinate axis was being calculated (those points correspond to the tier numbers n), this type of behavior (small and approximately exponentially decreasing population with the coordinate) could correspond to tunneling along the given coordinate axis. Hence, it can be said that the type of relaxation in our system is tunneling (or tunneling-like) along the tier coordinate.

It is relevant to comment on this behavior and to justify its being termed tunneling. This tunneling is not tunneling in its usual sense where the particle tunnels through a real potential energy barrier in coordinate space. The potential energy function

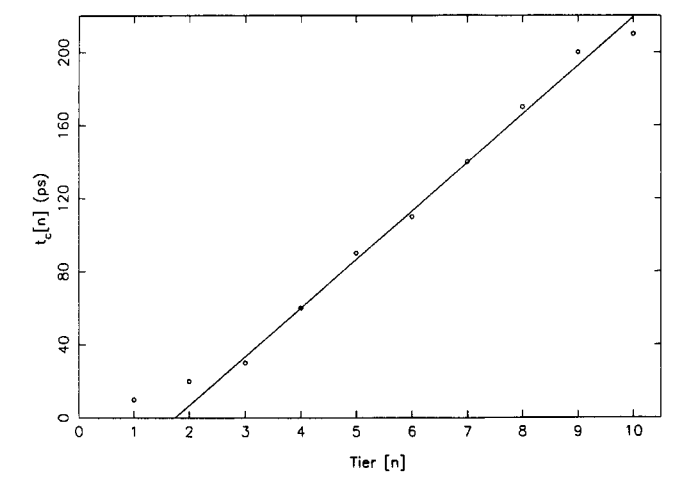


Figure 13. Threshold  $t_c^n$  as a linear function of tier number (n).

for our system is a multidimensional anharmonically distorted parabola, and there are no potential barriers separating different regions of the configuration space. The light state is, however, separated from the quasi-continuum of resonant states, in which the population ultimately flows, by many intermediate states which are well off-resonance. These states sequentially couple the light state and the quasi-continuum states.

This situation is much the same as in a superexchange model of the long distance electron transfer problem. The off-resonant states are the best resonances available in a given order of interaction (on the average, the frequency mismatch is much larger than the coupling). In classical mechanics those resonances cannot be used directly, and so the population can be locked into the initial CH state. One can say, hence, that the intermediate off-resonant states create a dynamical barrier for decay of the

Figure 14. Quasi-stationary populations (circles) and density of states (crosses) in intermediate tiers. Exponential approximation (linear curves in log scale) are shown by a solid and broken line, respectively. For the upper curve,  $W_n = P_i/P_{11}$  where  $P_i$  is the population of the *i*th tier and for the lower curve  $W_n = \rho_i/\rho_{11}$ , where  $\rho_i$  is the density of states in the *i*th tier.

CH vibration, even though there is no potential energy barrier. In the actual quantum system the population flows through this barrier in much the same way as usual quantum mechanical particle tunnels through the potential barrier. Thus, the tunneling occurs in our case under a dynamical barrier along the tier coordinate of the system. The connection of the superexchange type of vibrational coupling to dynamic tunneling has been recently discussed in detail by two of the present authors.<sup>21</sup> There are several examples of low-dimensional systems where this type of tunneling occurs. Perhaps, the two best examples of this phenomenon are the asymmetry doublet in the rotational spectra of the asymmetric tops<sup>22</sup> and doublets in the vibrational spectra of water (ref 21 and references therein). It should be added that the picture of tunneling between the invariant tori referred to earlier is only a rough approximation in these many-coordinate systems, since, as noted earlier, the tori are expected to be largely ruptured and other more complex modes of transfer<sup>16</sup> would then occur.

To understand the nature of the tier coordinate, it is useful to compare the results of our quantum calculation with what might be the classical or semiclassical analog of it. Action space is the most convenient representation for the relaxation dynamics in classical and semiclassical analysis. Each of the zeroth-order states of  $(CH_3)_3CCCH$  molecule is characterized by 3N-642 vibrational quantum numbers,  $|v_1, v_2, ..., v_{42}\rangle$ . For example, the light state CH with v = 1 is  $|1, 0, ..., 0\rangle$ . In the semiclassical analysis these quantum numbers correspond to zeroth-order actions divided by Planck's constant. Thus, each of the zerothorder states is represented by a point in the 42-dimensional action space of the molecule  $(I_1, I_2, ..., I_{42})$ . In the classical analysis these zeroth-order actions are not constants of the motion but rather are functions of time (only in a completely integrable system<sup>12,13</sup> are actions constants). The evolution of the system can be described as a classical trajectory in action space. In a semiclassical analysis the system is described by a wave function  $\psi(I_1,I_2,...,I_{42})$  in the same space. The population of a given zerothorder state corresponds to  $|\psi(I_1,I_2,...,I_{42})|^2$ . Initially all population is concentrated at a point corresponding to the light state. A detailed semiclassical description would involve the description of the time evolution of the total wave function  $\psi(I_1,I_2,...,I_{42})$ , or equivalently, the population of all vibrational states involved in the analysis. Instead, we focused on the total population of the tiers.

Qualitatively, the tier coordinate n is a measure of distance in action space from the light state to an average state belonging to the tier n. (n is exactly the order of coupling, described earlier, of the states in the tier to the light state.) Thus, the population

of the nth tier,  $P_n(t)$ , describes the total population of a particular region in action space, which is some distance away from the light state along the relaxation path.  $P_n(t)$  can also be regarded qualitatively as "radial" density of the total multidimensional wave function. Thus, the discussion of the dynamics in the present calculations is reduced to that along a one-dimensional tier coordinate. The qualitative picture that emerges from our calculations is as follows. Along the tier coordinate the initial distribution localized at  $P_0$  is separated from distant tiers by a dynamic barrier, a barrier in action space and not in the coordinate space in this case. The relaxation of the initial distribution can be regarded as due to tunneling through this barrier to regions where the quasi-resonant states are available. The population under the barrier is always very small, as in the usual case of tunneling under a potential barrier in coordinate space. Details of this tunneling relaxation dynamics have been the focus of various sections of this paper.

In many studies of the CH stretch relaxation it was suggested that the stretch-bend interaction plays the key role, because of a good 1:2 stretch-bend resonance<sup>20,23-25</sup> in case CH is attached to a rigid skeleton of a molecule, as, for example, in benzene<sup>20</sup> or in CX<sub>3</sub>H.<sup>23,25</sup> In the case of (CH<sub>3</sub>)<sub>3</sub>CCCH molecule the bend frequency is only of the order of 700 cm<sup>-1</sup>, because of the "soft" bend nature of the acetylenic part in the molecule. In this case the usual stretch-bend resonance does not play any significant role, at least in the present model where only low-order direct couplings are considered. In such a situation the high-frequency CH stretch is adiabatically separated from the rest of the lowfrequency modes of a molecule including the CH bend. Such a situation was discussed in the early eighties by Quack and coworkers.26 The superexchange type of vibrational couplings and tunneling provide the mechanism of relaxation out of such an adiabatic dynamical well.

#### V. Conclusions

We have demonstrated the mechanics of energy relaxation from a localized part of the molecule to its complete scrambling into all the available modes in the limit of statistical IVR when the decay is irreversible. This mechanism is explained within the tier formalism of sequential third-order anharmonic couplings that control the decay. The different roles played by the initial tiers when the average spacing between the states is larger than the average matrix elements and the later tiers where the density of states is high enough such that the statistical limit is reached have been demonstrated. We have also demonstrated that although the initial decay rate is a function of initial tiers only, the limit of irreversible decay is reached only in the presence of the quasi-continuum of states in the later tiers. Therefore, the irreversible decay occurs from the light states into the quasicontinuum mediated through the virtual couplings of the intermediate tiers. This mechanism clearly points out the importance of the intermediate tiers in the overall rate of relaxation and how bottlenecks in these tiers can significantly localize the excitation into the light state in spite of a large density of states available in the later tiers. This issue of localization versus statistical decay is discussed somewhere else<sup>10,27</sup> in detail. We have also identified an artifact of the dead-end state type and have indicated how to deal with it.

In this paper we have shown that the presence of virutal couplings in the intermediate tiers lead to superexchange between the light state and quasi-resonant states in the molecule. Dynamics of energy transfer resembles tunneling in tier space where the intermediate tiers never see a significant buildup of population. An intriguing behavior of the dynamics is shown in the threshold behavior. At very short times, when most of the population distribution is localized within the light state, some population moves along the tier coordinate such that the front of this population flow reaches successive tiers with a constant velocity. Once all the tiers have been reached, the irreversible decay out

of the initial tiers into the quasi-continuum can commence. If the tier structure is such that all the tiers cannot be reached then the probability of irreversible decay is substantially reduced.

Acknowledgment. A.A.S. thanks E. J. Heller, R. D. Levine, and M. Quack for helpful discussions and critical comments during the Berlin Conference where part of this work was presented. We are pleased to acknowledge the financial support of the National Science Foundation. This work is supported in part by the Caltech-JPL CRAY Supercomputing project. R.A.M. was asked to contribute to a volume in the *International Journal of Quantum Chemistry* dedicated to Professor I. Hjalmars-Fischer. We were not able to meet that deadline, but it is a pleasure to acknowledge her many important scientific contributions and to dedicate this article to her.

#### Appendix

The rapid decrease of population in the intermediate tiers with the tier index can be understood by invoking a standard argument from the high-order perturbation theory. The high-order corrections to the light state,  $|\phi_0\rangle$ , due to couplings to other state in the molecule can be written as

$$|\phi\rangle = |\phi_0\rangle + \sum_{k_1} c_{k_1} |\phi_{k_1}\rangle + \sum_{k_2} c_{k_2} |\phi_{k_2}\rangle + \dots \quad (A1)$$

where sums are taken over states in the first tier, second tier, etc. From standard perturbation theory arguments one finds

$$c_{k_1} = \left\langle \phi_{k_1} \middle| \frac{V}{E_0 - E_{k_1}} \middle| \phi_0 \right\rangle \tag{A2}$$

$$c_{k_2} = \sum_{k_1} \left\langle \phi_{k_2} \middle| \frac{V}{E_0 - E_{k_2}} \middle| \phi_{k_1} \middle\rangle \left\langle \phi_{k_1} \middle| \frac{V}{E_0 - E_{k_1}} \middle| \phi_0 \right\rangle \quad (A3)$$

$$c_{k_{n}} = \sum_{k_{n-1}} \left\langle \phi_{k_{n}} \frac{V}{E_{0} - E_{k_{n}}} \phi_{k_{n-1}} \right\rangle c_{k_{n-1}}$$
 (A4)

where V is the anharmonic coupling operator and  $E_k$  is the energy of the kth zeroth-order state. If one neglects interference effects and assumes that there are no strong resonances, then the population of a quasi-stationary state is given by

$$|c_{k_n}|^2 = \sum_{k_{n-1}} \left| \left\langle \phi_{k_n} \middle| \frac{V}{E_0 - E_{k_n}} \phi_{k_{n-1}} \right\rangle \right|^2 |c_{k_{n-1}}|^2$$
 (A5)

The population of the whole tier then can be written as

$$P_n = \sum_{k_n} |c_{k_n}|^2 = \sum_{k_{n-1}} \left( \sum_{k_n} \left| \frac{V_{k_n k_{n-1}}}{E_0 - E_k} \right|^2 \right) |c_{k_{n-1}}|^2$$
 (A6)

Thus one can write

$$P_n = \sum_{k} |c_k|^2 \simeq f P_{n-1} \tag{A7}$$

if one assumes that the factor f is roughly the same for the intermediate tiers

$$f = \sum_{k_n} \left| \frac{V_{k_n k_{n-1}}}{E_0 - E_k} \right|^2 \tag{A8}$$

It is thus seen that, if there are no resonant states in the sequence of tiers, the population decays roughly exponentially. For example

$$P_n = f^{n-3}P_3 \tag{A9}$$

The same type of mechanism explains the exponential distance

dependence of the electronic coupling in long-distance electrontransfer processes.

Of course, the above arguments hold only when there are no resonant states in the tier and the states are distributed in tiers more or less randomly. As the tier index increases, the density of states increases also increasing the chance to have good resonances. The above arguments, then, are not valid.

#### References and Notes

- (1) Stuchebrukhov, A. A.; Marcus, R. A. J. Chem. Phys. 1993, 98, 6044.
- (2) Kerstel, E. R. Th.; Lehmann, K. K.; Mentel, T. F.; Pate, B. H.; Scoles, G. J. Phys. Chem. 1991, 95, 8282.
- (3) Gambogi, J. E.; L'Esperance, R. P.; Lehmann, K. K.; Pate, B. H.; Scoles, G. J. Chem. Phys. 1993, 98, 1116.
- (4) Newton, M. D. Chem. Rev. 1991, 91, 767. Siddarth, P.; Marcus, R. A. J. Phys. Chem. 1992, 96, 3213.
- (5) Kramers, H. A. Physica 1934, I, 182. Anderson, P. W. Phys. Rev. 1950, 79, 350. McConnell, H. M. J. Phys. Chem. 1961, 35, 508.
  - (6) Wyatt, R. E. Adv. Chem. Phys. 1989, 73, 231.
- (7) Wyatt, R. E.; Iung, C.; Leforestier, C. J. Chem. Phys. 1992, 75, 3458. Wyatt, R. E.; Iung, C.; Leforestier, C. J. Chem. Phys. 1992, 75, 3477.
  - (8) Marshall, K. T.; Hutchinson, J. S. J. Chem. Phys. 1991, 95, 3232.
- Luckhaus, D.; Quack, M. Chem. Phys. Lett. 1992, 190, 511. Quack,
  M. Annu. Rev. Phys. Chem. 1990, 41, 839.
  - (10) Heller, E. J. Phys. Rev. A 1987, 34, 1360.
  - (11) Remacle, F.; Levine, R. D. J. Chem. Phys. 1993, 98, 2144.
- (12) Lichtenberg, A. J.; Lieberman, M. A. Regular and Stochastic Motion; Springer: New York, 1983.
  - (13) Uzer, T. Phys. Rep. 1991, 199, 73.
  - (14) Davis, M. J.; Heller, E. J. J. Phys. Chem. 1981, 85, 307.
- (15) Miller, W. H.; George, T. F. J. Chem. Phys. 1972, 56, 5668. George, T. F.; Miller, W. H. J. Chem. Phys. 1972, 57, 2458. Stine, J.; Marcus, R. A. Chem. Phys. Lett. 1972, 15, 536. Miller, W. H. Chem. Phys. Lett. 1974, 7, 431. Stine, J.; Marcus, R. A. Chem. Phys. Lett. 1974, 29, 575. Miller, W. H. Adv. Chem. Phys. 1974, 25, 69. Miller, W. H. Adv. Chem. Phys. 1975, 30, 77. Noid, D. W.; Marcus, R. A. J. Chem. Phys. 1977, 67, 559. Marcus, R. A.; Coltrin, M. E. J. Chem. Phys. 1977, 67, 2609. Lawton, R. T.; Child, M. S. Mol. Phys. 1979, 37, 1799. Babamov, V. K.; Marcus, R. A. J. Chem. Phys. 1981, 74, 1780. Davis, M. J.; Heller, E. J. J. Chem. Phys. 1981, 75, 3915. Sibert III, E. L.; Reinhardt, W. P.; Hynes, J. T. J. Chem. Phys. 1982, 77, 3583. Sibert III, E. L.; Hynes, J. T.; Reinhardt, W. P. J. Chem. Phys. 1982, 77, 5191. Shirts, R. B.; Reinhardt, W. P. J. Chem. Phys. 1982, 77, 5191. Shirts, R. B.; Reinhardt, W. P. J. Chem. Phys. 1982, 77, 5204. Noid, D. W.; Koszykowski, M. L.; Marcus, R. A. J. Chem. Phys. 1983, 78, 4018. Uzer, T.; Noid, D. W.; Marcus, R. A. J. Chem. Phys. 1983, 79, 4412. Conner, J. N. L.; Uzer T.; Marcus, R. A.; Smith, A. D. J. Chem. Phys. 1984, 80, 5095. Stefanski, K.; Pollak, E. J. Chem. Phys. 1987, 87, 1079.
- (16) Mackay, R. S.; Meiss, J. D.; Percival, J. C. Physica D 1984, 13, 55. Bensimon, D.; Kadanoff, L. P. Physica D 1984, 13, 82. Davis, M. J. J. Chem. Phys. 1985, 83, 1016. Davis, M. J.; Gray, S. K. J. Chem. Phys. 1986, 84, 5389. Gray, S. K.; Rice, S. A.; Davis, M. J. J. Phys. Chem. 1986, 90, 3470
  - (17) Zhang, Y.-F.; Marcus, R. A. J. Chem. Phys. 1992, 96, 6065.
- (18) Gordon, R. G. Adv. Magn. Reson. 1968, 3, 1. In eq 19 of this reference one substitutes  $\mu = \mu_{0g}|\phi_{0}\rangle\langle g| + \mu_{g}|g\rangle\langle\phi_{0}|$ , where  $|g\rangle$  is the ground vibrational state. Also  $E_{g} = \langle g|H|g\rangle$  is set equal to zero and  $\mu(t) = e^{tHt}\mu e^{-tHt}$ .
  - (19) Lehmann, K. K.; Pate, B. H. J. Mol. Spectrosc. 1990, 144, 443.
- (20) Sibert III, E. L.; Reinhardt, W. P.; Hynes, J. T. Chem. Phys. Lett. 1982, 92, 455. Sibert III, E. L.; Reinhardt, W. P.; Hynes, J. T. J. Phys. Chem. 1984, 81, 1115. Sibert III, E. L.; Hynes, J. T.; Reinhardt, W. P. J. Phys. Chem. 1984, 81, 1135.
  - (21) Stuchebrukhov, A. A.; Marcus, R. A. J. Chem. Phys. 1993, 98, 8443.
- (22) Harter, W. G.; Patterson, C. W. J. Chem. Phys. 1984, 80, 4241. Harter, W. G. J. Chem. Phys. 1985, 85, 5560.
  - (23) Dübal, H.-R.; Quack, M. J. Chem. Phys. 1984, 81, 3779.
  - (24) Halonen, L. J. Phys. Chem. 1988, 93, 3386.
- (25) Voth, G. A.; Marcus, R. A.; Zewail, A. H. J. Chem. Phys. 1984, 81, 5494.
- (26) von Puttkamer, K.; Dübal, H.-R.; Quack, M. Faraday Discuss. Chem. Soc. 1983, 75, 197
  - (27) Mehta, A.; Stuchebrukhov, A. A. Manuscript in preparation.